ELSEVIER

Nuclear Physics B (Proc. Suppl.) 77 (1999) 171–176

NUCLEAR PHYSICS B
PROCEEDINGS
SUPPLEMENTS

Present Status of KamLAND

A. Suzuki
(for the KamLAND Collaboration)

Research Center for Neutrino Science, Tohoku University,
Aoba, Sendai 980-8578, Japan

The KamLAND project, a 1000 ton Kamioka Liquid scintillator AntiNeutrino Detector, started in 1997. Fundamental designs of the detector components have been almost finished. Civil engineering works are ready in June this year. The data-taking is expected to begin in January 2001.

1. INTRODUCTION

To research for the physics and astrophysics of neutrinos by means of detecting lower energy terrestrial and extra-terrestrial neutrinos and anti-neutrinos, the project of a 1000 ton liquid scintillator experiment, KamLAND was proposed in 1994. After the detector R&D, it was approved in 1997 [1]. Since 1998, the KamLAND project has been performed by the Japan and U.S. collaboration. Primary targets of physics in KamLAND are to search for neutrino oscillations in $\Delta m^2 > 10^{-5}$ eV^2 with reactor anti-neutrinos, to aim at the first observation of geoneutrinos, and to study neutrions from possible supernovae explosions. We are also contemplating a second phase of data-taking that, through improvements in the liquid scintillator purification will allow us to observe the ^{8}B and ^{7}Be solar neutrinos.

2. KamLAND DETECTOR

The KamLAND detector sits at the old Kamiokande site, dismantling the Kamiokande detector. The rock overburden is more than 2700 m.w.e. in any direction. The expected cosmic-ray muon rate for the detector is 0.3 Hz. The rock cavity is enlarged by 4 m in depth from the present bottom level. The site also includes the counting facilities, water and scintillator purification systems, ventilation system and electrical power station.

The detector consists of 3 layers as illustrated in Fig. 1. The cylindrical rock cavity with a 20 m diameter and a 20 m height is covered with waterproof lining materials in order to use as a water Cherenkov anti-counter. The inside of the anti-counter is segmented into small rooms by light reflection sheets so as to identify an entrance and exit points of incoming cosmic-ray muons. The old Kamiokande 20 inch-photomultiplier tubes (PMT's) are reused in this counter. A stainless steel spherical buffer tank with a 18 m diameter is solidly mounted inside the anti-counter. Mineral oil is filled into the tank to reduce buoyancy applied to the innermost liquid scintillator layer. 1280 newly developed 17 inch-PMT's are attached onto the entire inner surface of this tank, which gives 22 % photosensitive coverage. The 17 inch-PMT has the same shape and size as those of the 20 inch-PMT, but only a central part of photocathode is available. The dynode structure is a box-and-line type instead of a venecian-blind. As a result, under the conditions of single photoelectron illumination, 10^7 gain and 25 °C, a good time-resolution and a clear isolated pulse-shape are obtained: Transit Time Spread of (1-1.5) ns for 1 σ; Peak to Valley ratio of (3-5); and Dark counting rate above 0.25 photoelectron (p.e.) of 10 kHz on average. A proper operation of the PMT's is assured in the < 50 mGauss field which is realized by a set of compensating coils installed in the cavern to cancel the Earth's magnetic field.

PII S0920-5632(99)00414-4

A 1200 m^3 plastic balloon containing $\sim$ 1000 ton liquid scintillator is deployed inside the buffer tank. A multi-layer film made of nylon + EVOH (poly vinyl alcohol) + nylon is a candidate balloon material. The EVOH film has low Radon permeability of $< 10^{-10}$ cm/s [2]. Scintillator cocktail which is made of 80% concentration of isoparaffin, 20% of pseudocumene and 2g/l of fluor (PPO), was chosen to keep the flash point greater than 60 °C. Such scintillator shows the following properties: more than 50 % of the Anthracene light output; 10 m and 20 m of the light attenuation length for 400 nm and 450 nm light, respectively; 90 % of the neutron rejection from γ-like signals; and (13.7 $\pm$ 2.1) of the α-particle quenching factor. We expect $\sim$ 100 p.e. /MeV in KamLAND, which gives $\sigma(E)/E \sim 10\ \%/\sqrt{E}$. Contamination of U and Th in the liquid scintillator have been measured by a ICP-mass separator. Without purifying, the scintillator cocktail includes 2×10^{-13} g/g of U and $< 6 \times 10^{-12}$ g/g of Th. Our Monte Carlo study tells us that 1 order of magnitude reduction both for U and Th is required in the reactor neutrino oscillation search and more than (3-4) order of magnitude in the solar neutrino detection.

Figure 1. Schematic view of the KamLAND detector.

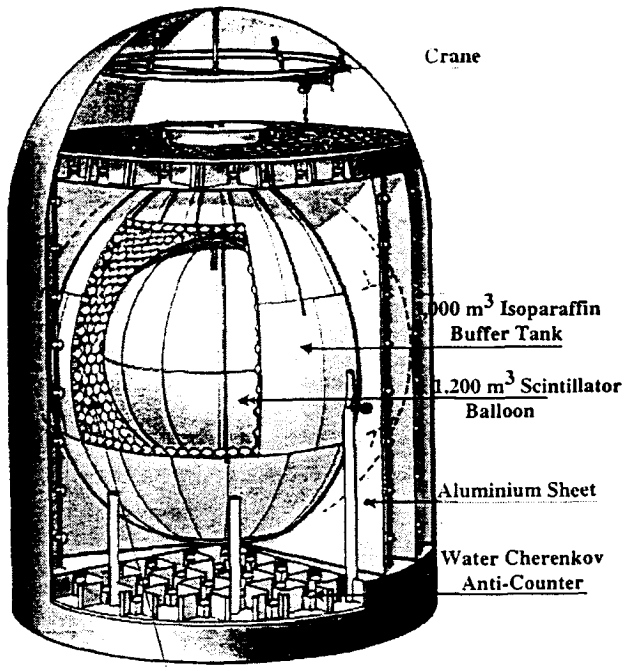

3. PHYSICS GOALS

3.1. Long baseline neutrino oscillation search

Neutrino oscillation searches in KamLAND are carried out using nuclear reactors. Anti-neutrinos produced in reactors are measured by detecting the inverse β-decay process (E_{th} = 1.8 MeV), $\bar{\nu}_e p \rightarrow e^+ n$ with the aid of a timing coincidence between a prompt e^+ signal and a delayed γ (2.2 MeV) coming from a thermal neutron capture on a proton. There are several commercial nuclear power plants around the Kamiokande site. An anti-neutrino flux of $1 \times 10^6 cm^{-2} s^{-1}$ is expected for $E_{\bar{\nu}} > 1.8$ MeV. 80 % of such flux derives from reactors at a distance between 140 km and 210 km. Thus, the flight range is limited in spite of using multi-reactors. A total thermal power flux is found to be change by at least 30 % season to season due to the high power consuming in summer and winter, and the obligatory 3 months maintenance in spring or fall .

About 450 $\bar{\nu}_e p \rightarrow e^+ n$ events for one year running are expected with the 600 ton fiducial mass. On the other hand the correlated (with the timing coincidence) background event rate is estimated to be 8 in a year, assuming 10^{-14} g/g for U and Th, 10^{-12} g/g for K and 0.5 mBq/m^3 for Rn concentrations in the liquid scintillator. Fig. 2 shows the expected positron energy spectrum together with that of background events. One can see no serious effect from backgrounds.

There can be carried out three different oscillation analyses by (A) measuring the absolute flux, (B) the spectrum change and (C) the seasonal flux variation. Sensitivity of these three methods is depicted in Fig. 3, where a solid curve is obtained from (A) for 1 year data, a dotted one from (B) for 5 years data and a dashed one from (C) for 5 years data. An accessible oscillation parameter space is reached to $\Delta m^2 \sim 10^{-5}$ eV^2 and $\sin^2 2\Theta > 0.1$. This improves the present sensitivity [3] by over 2 order of magnitude and covers the MSW large angle solution to the solar neutrino deficit.

Figure 2. Expected positron energy spectra from reactor anti-neutrinos and backgrounds.

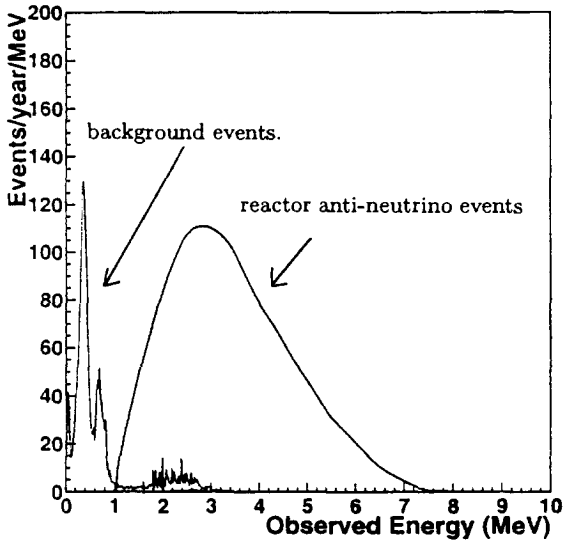

Figure 3: Parameter constraints on $\nu_e \rightarrow \nu_x$ oscillations. The solid contour represents the 95 % C.L. from the absolute flux change, the dotted contour the 90 % C.L. from the spectrum shape chage, and the dashed contour the 85 % C.L. from the seasonal flux variation. The shaded region shows the MSW large mixing solution.

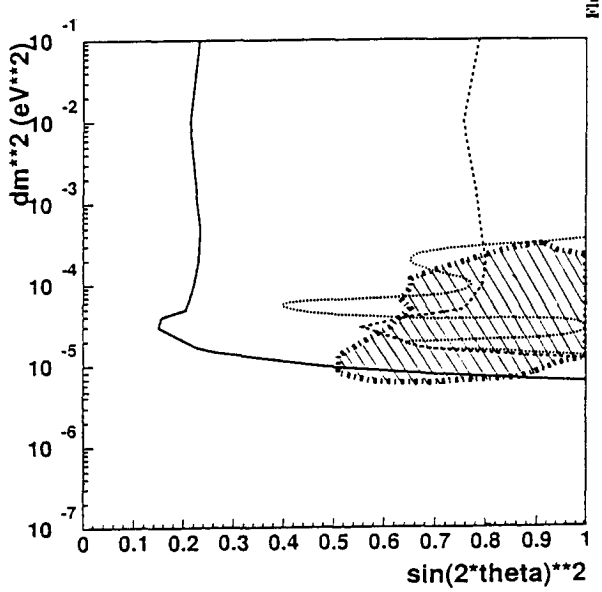

3.2. Geoneutrino detection

A first chance for terrestrial $\bar{\nu}_e$ (geoneutrino) search [4] [5] can be expected in KamLAND. A basic factor in the interior dynamics and the evolution of the present Earth is the radiogenic heat mainly from U and Th decays inside the Earth. Measuring the U and Th concentrations in the Earth interior sheds new light on geophysics. Calculation of the geoneutrino flux strongly depends on models concerning the abundance of U and Th in the continental crust, oceanic crust, upper-mantle and lower mantle. Fig. 4 is one example of the flux calculation by Krauss *et al.* [6]. Geoneutrinos are measured by the same method as reactor anti-neutrinos through a timing coincidence. For energies above the inverse β-decay threshold, 1.8 MeV only the U and U+Th components are separately detectable as seen in Fig. 4.

Figure 4. Geoneutrino flux calculation [6].

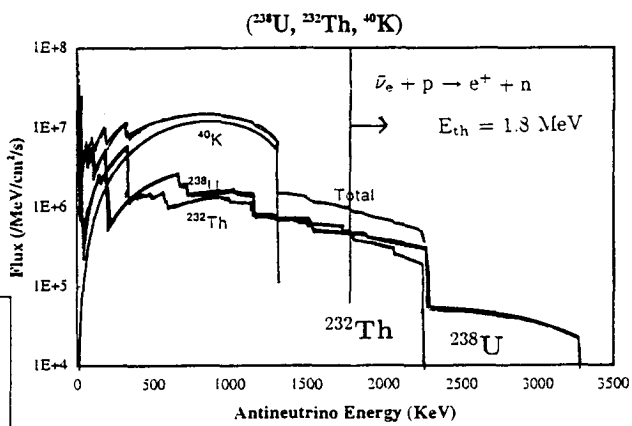

The energy spectrum of geoneutrino events estimated using some models on the U and Th abundance is shown in Fig. 5, being superimposed on the reactor signals [7]. Characteristic point is that neutrinos from β-decays of heavy nuclei possess their energies near the maximum energy end. This is due to the large Coulomb screening effect on an accompanying electron. Thus, one can see clear and sharp peaks of the U and U+Th components standing on the continuous reactor anti-neutrino signals. More than several tens of geoneutrino events can be expected for one year operation in KamLAND.

Figure 5. Positron energy spectrum induced by geoneutrinos and reactor anti-neutrinos [7].

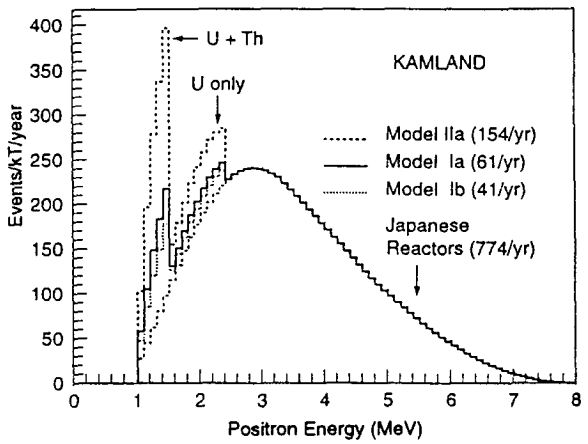

3.3. Observation of galactic supernova neutrino bursts

Through neutrino and anti-neutrino interactions with free protons and carbon nuclei, new windows in the detection of supernova neutrino bursts are opened in KamLAND. The number of events expected in a galactic supernova burst is calculated, taking the following typical parameters: the distance of 10 kpc; the released energy of 3×10^{53} erg; and the temperatures of 3.5 MeV ($< E_\nu > = 11$ MeV) for ν_e, 5 MeV ($< E_\nu > =$ 16 MeV) for $\bar{\nu}_e$ and 8 MeV ($< E_\nu > = 25$ MeV) for $\nu_\mu, \bar{\nu}_\mu, \nu_\tau, \bar{\nu}_\tau$ [8]. Table 1 gives the expected number of events for different reaction channels.

The direction of the exploded star is determined by 16 single electron events from the neutrino-electron scattering. The Monte Carlo study shows that a Cherenkov ring produced by electrons with their energies above 10 MeV can be found out among scintillation light. If the distance is known, the neutrino luminosity of the supernova is obtained by 330 inverse β-decay events which are recognized by the same method as the reactor anti-neutrino detection. 58 events are expected from the neutral current reaction on ^{12}C, in which the 15.11 MeV monochromatic γ-ray is produced from the ^{12}C excited state. This gives a sensitive monitor of the supernova neutrino temperature, if the distance and the neutrino luminosity are known. Fig. 6 is the visible energy distribution of the inverse β-decay events and the neutral current events.

Table 1. Expected rates in KamLAND for a galactic supernova neutrino burst

reactions			no. of events
$\nu_x(\bar{\nu}_x)e^-$	$\rightarrow$	$\nu_x(\bar{\nu}_x)e^-$	16
$\bar{\nu}_e$ p	$\rightarrow$	e^+ n	330
$\nu_e{}^{12}$C	$\rightarrow$	e^- ^{12}N	2
$\bar{\nu}_e{}^{12}$C	$\rightarrow$	e^+ ^{12}B	7
$\nu_x(\bar{\nu}_x)^{12}$C	$\rightarrow$	$\nu_x(\bar{\nu}_x)^{12}$C*	58

E(^{12}C*) = 15.11 MeV

Figure 6. Visible energy spectrum of $\bar{\nu}_e$ p $\rightarrow e^+$n and $\nu_x(\bar{\nu}_x)^{12}$C $\rightarrow \nu_x(\bar{\nu}_x)^{12}$C* events [8].

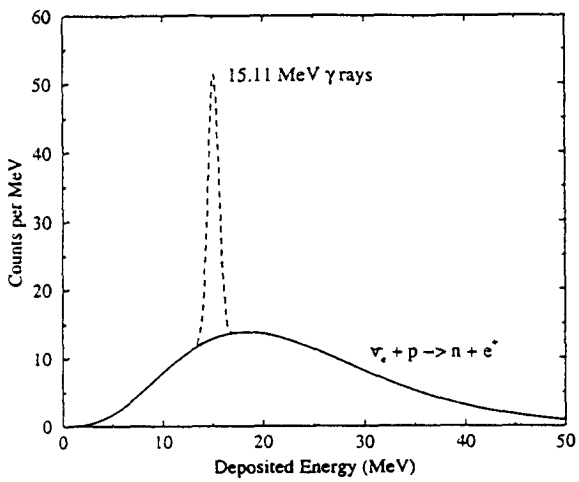

Nuclear excitation events induced by the charged current interactions, ν_e ^{12}C $\rightarrow$ e^- ^{12}N and $\bar{\nu}_e$ ^{12}C $\rightarrow$ e^+ ^{12}B, are measured by applying the time and space correlations between the prompt e^- (e^+) and delayed decaying $e^+(e^-)$ from the β unstable ground state of ^{12}N (^{12}B). Thus they are essentially background free. These two processes provide a unique test of two neutrino oscillation solutions to solve the solar neutrino deficit. The "Just So" solution gives 14 events each for the ν_e ^{12}C $\rightarrow$ e^- ^{12}N and $\bar{\nu}_e$ ^{12}C $\rightarrow$ e^+ ^{12}B channels. The MSW solution gives 27 events for the

ν_e $^{12}C \rightarrow e^-$ ^{12}N channel instead of 2 events, but no change in the $\bar{\nu}_e$ $^{12}C \rightarrow e^+$ ^{12}B channel. This would be a chance to determine the solution of the solar neutrino deficit.

3.4. Solar neutrino detection

The physics considered above can be achieved in the first stage KamLAND experiment with existing technology. In the next step we aim to explore the "sub-MeV" physics. Since the ν e $\rightarrow \nu$ e scatterings, involving single ionization events are dominant in this energy region, the experiment in the ultra-low background environment is required substantially. Pioneering works have been already done in Borexino and demonstrated the feasibility of the low background liquid scintillator experiment to this research field [9].

The energy sensitivity of $\sim$ 110 p.e./MeV in KamLAND makes it possible to set a detection threshold energy of $\sim$ 300 keV. Hence the ^{8}B and ^{7}Be solar neutrinos can be measured in principle. A skillful purification of the liquid scintillator, quite low Rn invading into the scintillator fluid, keeping the detector clean in construction and a large shielding volume for external backgrounds make it possible to detect the ^{8}B and ^{7}Be solar neutrinos in KamLAND in future.

Fig. 7 shows the expected recoil-electron energy spectrum of solar neutrino events together with the spectrum of backgrounds. 940 ^{8}B events/year with energy > 4 MeV and 110 ^{7}Be events/day with energy > 0.3 MeV are expected for the 560 ton and the 300 ton fiducial mass, respectively. The background spectrum is calculated assuming 10^{-16} g/g for U and Th, 10^{-14} g/g for K and 10 μBq/m^3 for Rn in the liquid scintillator and by quoting the data of radioactivity measurements of the detector materials and rocks. Under such a low background level the spectrum down to 3.5 MeV for the ^{8}B events is detectable, which is essential to examine whether the solar neutrino deficit is given rise to the MSW small angle or the "Just So" oscillation. The ^{7}Be signal also exceeds over the background one. This gives us variety tests on solutions to the solar neutrino problem [9]. Considering 0 SNU for the ^{7}Be neutrino observation obtained by the on-going experiments, it would be invaluable to measure the ^{7}Be neutrinos independently in Borexino and KamLAND.

Figure 7. Expected energy spectra of solar neutrino events and background events.

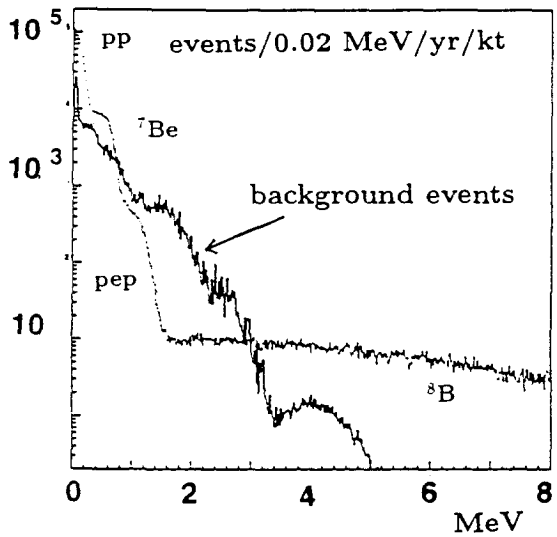

3.5. Higher energy physics

Although the first priority of the KamLAND physics is charged in "MeV" and "sub-MeV", the KamLAND detector performance allows to measure the "MeV - GeV" events. Energy response of the new 17 inch-PMT's is quite well in using at 10^7 gain as seen in Fig. 8. Here one can see not only a linear response up to 1,000 p.e., but also no saturation even at 10,000 p.e. This means the energy deposited by cosmic-ray muons passing through the detector is measurable. So recoil-protons produced by the neutral current interactions of the atmospheric neutrinos and the decays of charged pions and kaons produced in the atmospheric neutrino interactions and proton decays are identified with the aid of wave-form digitizers in the KamLAND front-end electronics.

4. Conclusions

KamLAND was approved by a 5 year project since 1997 of the JSPS program . Hence the construction schedule is so tight as shown below. All the Kamiokande detector components belonged in Tohoku Univ. in March 1998, partly from ICRR, Univ. of Tokyo and partly from KEK. Then civil engineering works at the mine side have been following since June.

Figure 8. Range of anode-current linearity of the new 17 inch-PMT at 10^7 gain as a function of light flux in units of p.e.

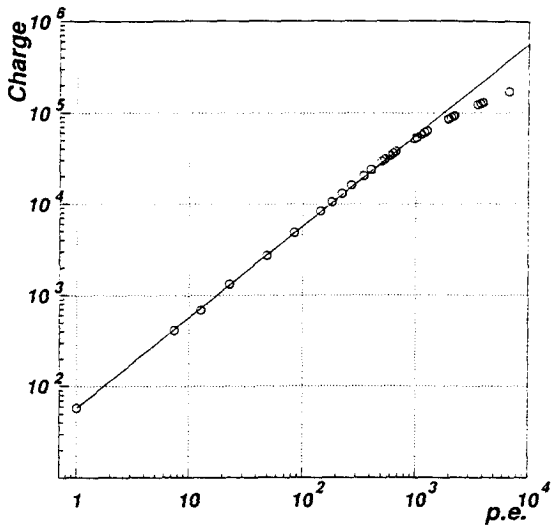

In 1998

- Remove the Kamiokande detector and expand the tunnel size and detector doom depth,
- Construct the 5,400 m^3 water pool for the water Cherenkov anti-counter;

In 1999

- Construct the 3,000 m^3 spherical buffer tank,
- Install 1280 17" PMT's into the buffer tank,
- Deploy the 1200 m^3 plastic balloon,
- Construct the water and liquid scintillator purification systems;

In 2000

- Install data taking electronics and computers,
- Fill 1000 ton liquid scintillator inside the balloon,
- Prepare and adjust all equipments; and

In 2001

- Start data taking in January 1.

We are grateful to Dr. R. Raghavan for valuable discussions and suggestions since planing this project and to Dr. M. Chen for discussions and measuring Rn permeability. We also would like to thank for discussions to the KamLAND collaborators: P. Alivisatos, S. Berridge, N. Bokor, C. Britton, W. Bryan, W. Bugg, J. Busenitz, T. Chikamatsu, H. Cohn, L. DeBraeckeleer, B. Dieterle, Yu. Efremenko, S. Enomoto, K. Furuno, S. Frank, C.R. Gould, G. Gratta, H. Hanada, E. Hart, S. Hatakeyama, G. Horton-Smith, T. Itoh, T. Iwamoto, Yu. Kamyshkov, S. Kawakami, M. Koga, J. Kornis, K.B. Lee, H.L. Liew, K. Mashiko, L. Miller, M. Nakajima, T. Nakajima, A. Nemeth, V. Novikov, H. Ogawa, K. Oki, P. Pacher, A. Piepke, S. Riley, N. Sleep, J. Shirai, F. Suekane, A. Suzuki, O. Tajima, K. Tagashira, T. Takayama, K. Tamae, H. Tanaka, D. Takagi, T. Taniguchi, W. Tornow, D. Tracy, P. Vogel, Y-F. Wang, H. Watanabe, A. Wintenberg, J. Wolf and J. Wolker. .

REFERENCES

[1] The KamLAND project is supported by Center of Excellence Grant of JSPS (Japan Society for the Promotion of Science).

[2] M. Chen, private communication (1998)

[3] M. Apollonio *et al.*, Phys. Lett., B420 (1998) 397.

[4] G. Eder, Nucl. Phys., 78 (1966) 657.

[5] G. Marx, Czech. J. of Phys., B19 (1969) 1471.

[6] L. M. Krauss, S. L. Glashow and D. N. Schramm, Nature, 310 (1984) 191.

[7] R. S. Raghavan, S. Schoenert, S. Enomoto, J. Shirai, F. Suekane and A.Suzuki, Phys. Rev. Lett., 80 (1998) 635.

[8] P. Vogel, private communication; The KamLAND proposal, Stanford-HEP-98-03, Tohoku-RCνS-98-15, (1998).

[9] L. Oberauer, Talk in this conference (1998).